8

Relating Crustal Structure and Stress Indicators in the Azores Islands

Nuno Dias[1,2] and Luís Matias[2,3]

[1]*Instituto D. Luiz,*
[2]*Instituto Superior Engenharia de Lisboa,*
[3]*Faculty of Sciences, University of Lisbon*
Portugal

1. Introduction

The Azores Archipelago is a region of intense geodynamical activity, with particular morphology and tectonics, which results in an intense seismic and volcanic activity (cf. Fig. 1). The seismic activity recorded in the region is very high, predominating low magnitude events organized in space and time in seismic crisis, sometimes triggered by stronger

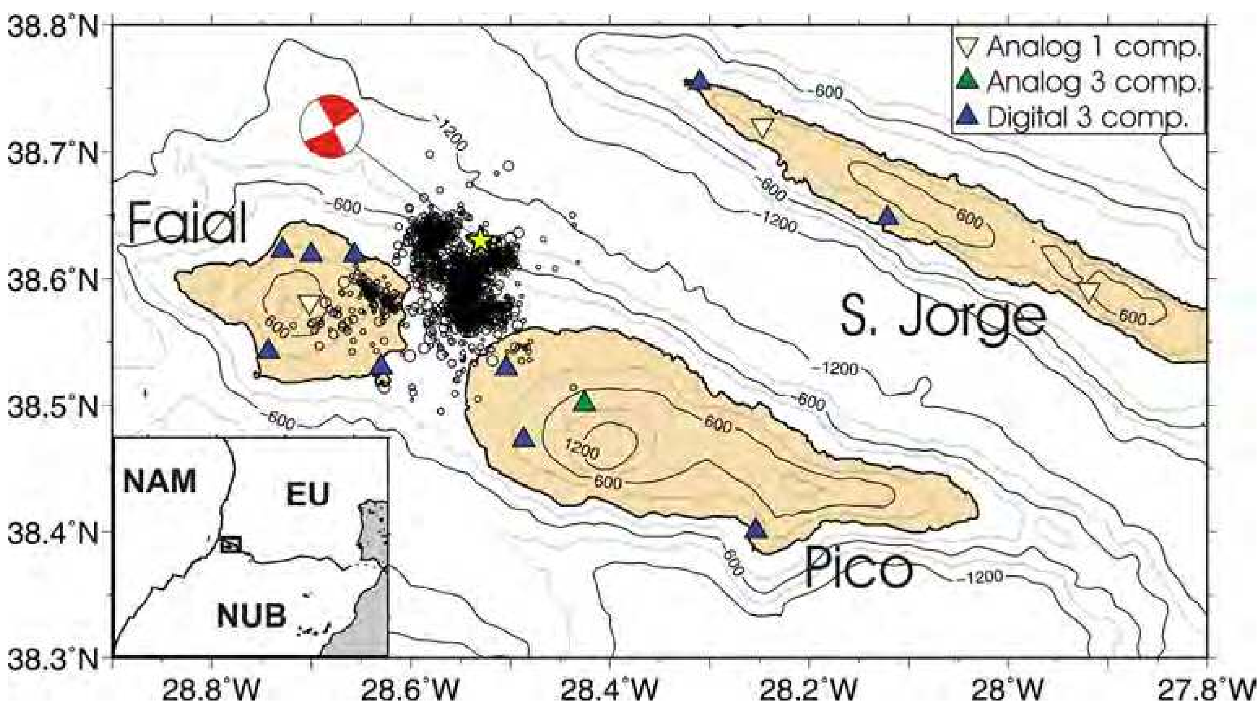

Fig. 1. Epicentral distribution of the aftershocks recorded between 9 and 31 of July 1998, located with MAC model (Senos et al., 1980). The Harvard-CMT focal mechanism is showed, pointing to the main shock location. Location of SIVISA permanent seismic stations and the temporary portable stations of IM and IGIDL/CGUL as triangles. Isobaths interval of 300m (Lourenço et al., 1998). Inset: Azores Triple Junction between North-America, Eurasia and Nubia plates.

earthquakes such as the 1980 (Ml~7.2) Terceira earthquake or the 1998 (Ml~5.8) Faial earthquake. Besides the interest of such a natural laboratory for Geosciences, the study and understanding of such phenomena is also critical in terms of civil protection and associated risk assessment, because such seismic activity has often a significant impact in economic and human terms. However, the available knowledge on the mechanisms responsible for the observed seismicity pattern and its relationship with tectonic and volcanic features of the region is still unsatisfactory.

The occurrence of the July 9th 1998 earthquake near the island of Faial, together with the fact that the instrumental coverage of the seismic sequence generated by this earthquake applied for the first time digital seismic stations, opened a window of opportunity for a comprehensive analysis on the mechanisms involved in the generation of such seismicity. The main event triggered a seismic crisis of thousands of aftershocks, strongly monitored in the weeks following the event, whose analysis allowed defining the characteristics of such seismicity and its relationship with volcanic and tectonic phenomena associated with the Tectonic Triple Junction environment.

The analysis of the aftershocks aimed at one hand the spatiotemporal characterization, by reviewing and refining the hypocentral locations, the determination of the seismic generation mechanisms and identification of the main active structures (Dias, 2005; Matias et al., 2007); on the other hand, to determine the crustal structure, with the refinement of the existing 1-D models, determining the local three-dimensional structure, analysis of seismic anisotropy and correlation with the state of crustal stress (Dias, 2005; Dias et al., 2007).

2. Temporary seismic network and data selection

At the time of the July 9th 1998 earthquake, the existing permanent seismic network of SIVISA (Seismological Surveillance System of Azores) was composed by 17 analog single-component (vertical) stations and 8 three-component analog stations, all with A/D converters, plus 4 digital stations. All stations were short-period, the analog stations - equipped with MARK L4C seismometers of 0.5 s (2 Hz) and the digitals with Lennartz LE-3D seismometers, 1 Hz. The only exception was the broad-band station of CMLA in São Miguel island, belonging to the worldwide network IRIS/IDA, equipped with a very broad-band triaxial Streckeisen STS-2 seismometer. This network was installed in 8 islands of the Azores Archipelago.

In the days following the main earthquake, the Meteorology Institute (IM), the Infante D. Luíz Geophysical Institute (IGIDL) and the Geophysical Centre of the University of Lisbon (CGUL)[1], in order to improve the instrumental coverage of the aftershocks by the SIVISA permanent network, deployed several portable digital seismic stations: IM placed 5 stations on Faial and Pico islands, while 2 additional stations were placed by IGIDL-CGUL on S. Jorge island. The seismometers used on all temporary stations were Lennartz LE-3D sensors, analogue to those used in the permanent digital stations. This increased the seismic monitoring network to a total of 14 stations located on the three islands surrounding the epicentral area (cf. Fig. 1). The stations sampling rates were 100 Hz for the IGIDL-CGUL stations, 125 Hz for IM stations; due to limited storage capacity, the data recorded by the 5 IM temporary stations were latter decimated to half, being stored with 62.5 Hz.

The temporary stations were operational until the end of July 1998, allowing a significant increase in the network registering capability, lowering the magnitude detection threshold

[1] IGIDL and CGUL were latter merged into Institute D. Luiz (IDL).

to events between 0.9 and 1.1 ML (Dias, 2005). During this period thousands of events were detected, with 4627 located aftershocks (Matias et al., 2007).
In order to maximize the quality and reliability of the results, for the one-dimensional modelling a set of 692 events was selected with the following criteria (Dias, 2005; Matias et al., 2007): minimum number of 6 stations recording an event, with one station at least located on S. Jorge island and azimuthal gap (GAP) smaller than 180º. For the 3-D modelling and seismic anisotropy analysis the criteria were more severe, with the used data set reduced to 688 and 438 events, respectively.

3. Tomographic inversion and crustal seismic structure

The inversion of a 1-D or 3-D seismic model of the crustal structure is based on the source-station travel times of seismic waves, generally by minimizing the time residual (difference between observed and theoretical travel times) due to disturbances introduced in the hypocentral coordinates and model properties. The dependence or coupling between the hypocentral parameters and the velocity structure being modelled is usually resolved by way of damped least-squares (Menke, 1984); a more detailed discussion on these methodologies can be found at Thurber (1993), Kissling et al. (1994), Thurber et al. (2000) or Thurber (2003). The resolution of this coupling problem requires the use of seismic events with stable hypocentral solutions, a criterion which must be balanced with the best spatial coverage possible (Thurber, 1993; Kissling et al., 1994; Thurber et al., 1999).
The methods used for the inversion of the velocity structure are implemented in programs like VELEST (Kissling et al., 1994; Kissling, 1995) for 1-D structure and SIMUL2000/SIMULPS (Thurber, 1983; Thurber et al., 1999) for 3-D structure. In the first case the model is parameterized by plane horizontal layers where seismic properties like P-wave velocity, Vp, or the Vp/Vs ratio remain constant, while in the former the model parameterization is done using a three-dimensional grid where on each node the value of these properties is set, with the values in other regions obtained by linear interpolation. Given the lower quality usually associated with S-waves readings compared to P-waves, both methods invert directly to the Vp and Vp/Vs structures, the Vs structure being latter derived from them.
Figure 2 displays the best (minimum) 1-D model obtained for the area between the islands of Faial, Pico and São Jorge, labelled FAIAL98 (Matias et al., 2007). Considering the P and S velocities and the Vp/Vs ratio of the model, and comparing with values associated with typical oceanic crusts (Tanimoto, 1995; Karson, 1998) it is possible to make a generic interpretation in petrological terms of the crustal structure of the area under study. The results indicate a basaltic composition for the layer located between 1 and 3 km in depth (Layer 2), with the velocities values suggesting a succession from lava flows to pillow lava and basaltic dikes. Between 3 and 12.5 km, the values of Vp and Vp/Vs indicate the presence of a Layer 3 with increased thickness, whose composition corresponds to Gabbro type mafic rocks. The location of the Moho at 12.5 km is an effect arising from the numerical modelling, the crust-mantle transition being more gradual and located between 12 and 14 km depth. The Moho associated Vp values will be intermediate values between 7.3 and 7.7 km/s, a possible evidence of a gradual increase of ultra-mafic rocks intrusion in the lower crust or the effect of variations in the depth of the Moho.

In order to determine the 3-D crustal structure in the tomographic inversion process (Dias et al. 2007) the above 1-D model was used as initial model, parameterized in the 3-D grid of Figure 3. After relocation of the earthquakes used in the 1-D modelling, the stability criteria for the hypocentral solutions were strengthened, with only 688 events used (cf. Fig. 3).

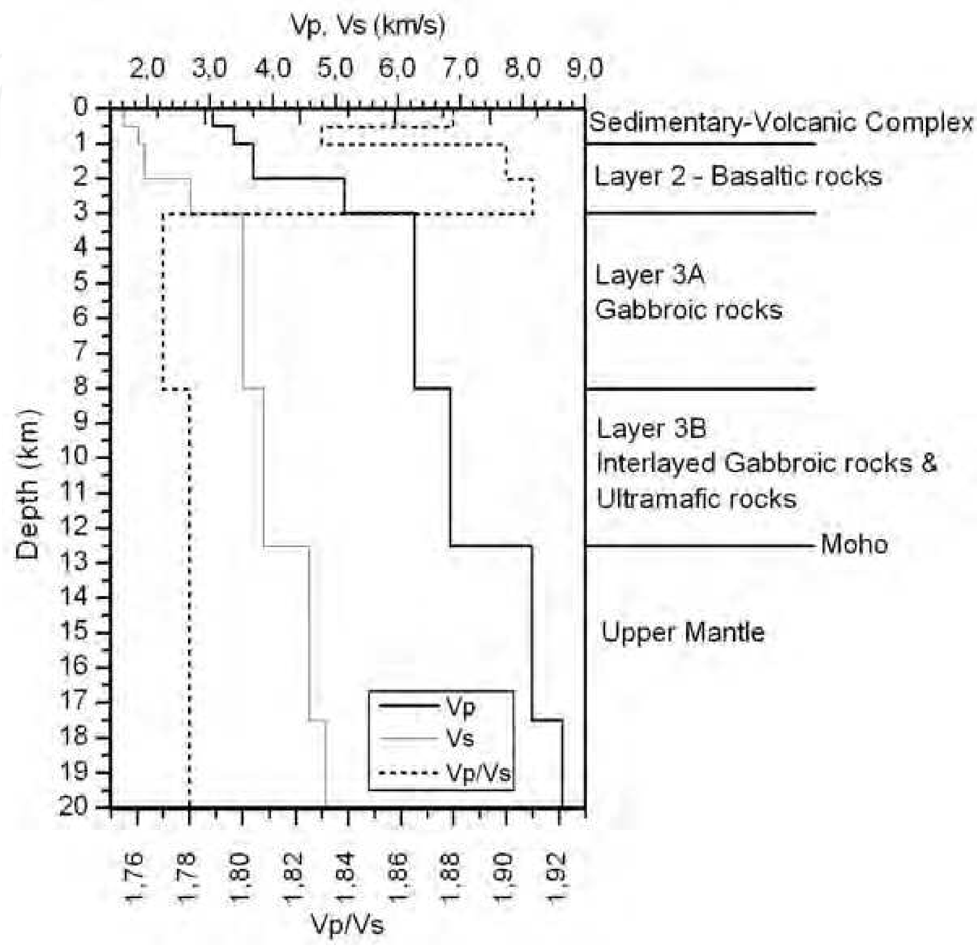

Fig. 2. Vertical profiles of P and S waves velocities and Vp/Vs ratio distribution corresponding to the new 1-D model FAIAL98, together with its petrological interpretation (Dias, 2005; Matias et al., 2007).

Any tomographic modelling process leads to a mathematic solution where it is important to estimate the quality of such solution in physical terms, namely by defining the regions of the model that can be considered well resolved. This evaluation can be accomplished through analysis of mathematical parameters related to the model resolution, reflecting the distribution of information and associated resolution, and also by performing sensitivity tests that use synthetic models or data. Only after such tests were performed, and together with joint analysis of the resolution parameters, is possible to define the resolved areas that will later be interpreted in physical terms. For discussion on the tomographic resolution of tomographic models see for example Menke (1984), Eberhart-Phillips (1993), Kissling et al. (1994), or Kissling et al. (2001); for the quality assessment of the model presented here see Dias (2005) and Dias et al. (2007).

Figure 4 shows the tomographic model obtained, in horizontal planes of Vp and Vp/Vs structures at depth, with resolved areas outlined. Given the information distribution (source-station paths), the resolved areas are located around the NNW area of the Faial -Pico channel and essentially between depths of 4 to 10 km. At the shallower level (1.0 km) there is good agreement between the anomalies of the tomographic model and the surface geological structure, particularly with the several volcanic units, but the most relevant feature of the tomographic model is the presence of a high-velocity body (Vp>6.3 km/s) located under the NW area of the island of Faial and extending from 6-7 km to a depth of approximately 13 km, which is enclosed in the northeast and east by deeper seismicity.

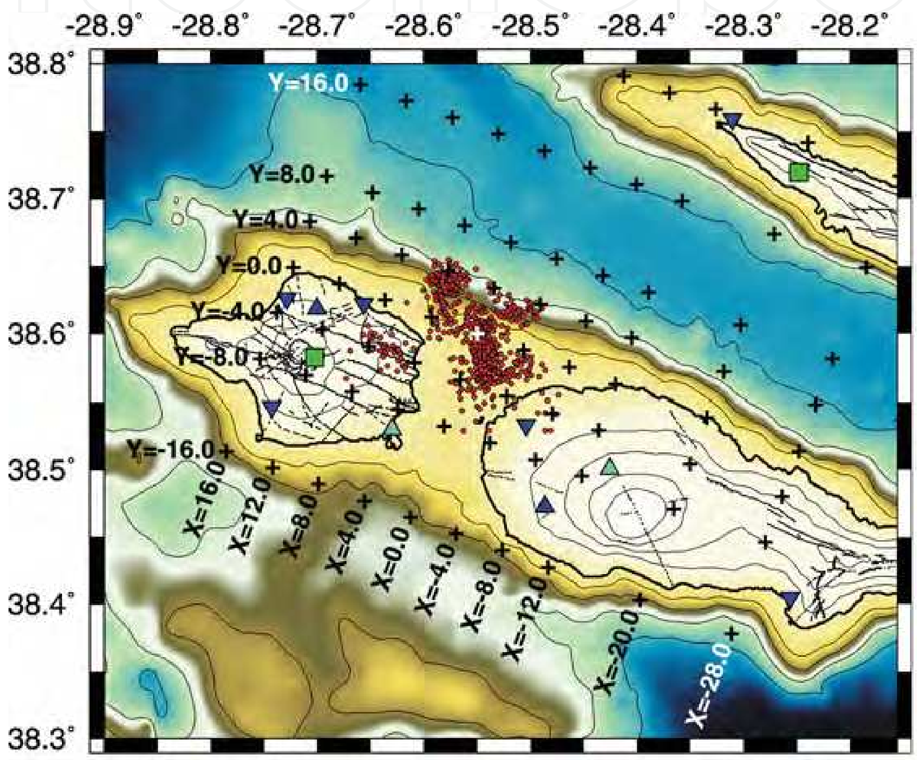

Fig. 3. Horizontal grid nodes positions (crosses) of the 3-D grid, seismic network (cf. Fig. 1) and epicenters (red dots) of the 688 selected events. A white cross marks the center of the grid, and the X and Y coordinates of Figure 4 are represented laterally to the grid. The horizontal distance between nodes was of 4-8 km, and vertically the nodes were placed in layers located at depths Z = 1, 4, 7, 10, 13, 17 km.

In the deepest levels (Z = 7, 10 km, see Figure 4) there is a strong lateral gradient to NNE in the direction of the S. Jorge channel, mainly of the Vp/Vs ratio that drops from 1.82 to less than 1.72; since this transition is partly coincident with the NNE limit of the high-velocity body and simultaneously runs parallel to the Faial-Pico alignment, it probably reflects the presence of an important tectonic feature. Under the central area of Faial, there is the presence of a low velocity zone (Vp <6.0 km/s), with a 5-10% lateral gradient on Vp and extending between 4 and 7 km in depth; under Pico there is the suggestion of the presence of a similar anomaly. The location of these anomalies is consistent with the estimated position for the magmatic chambers of the main volcanic edifices of Faial and Pico (Machado et al., 1994).

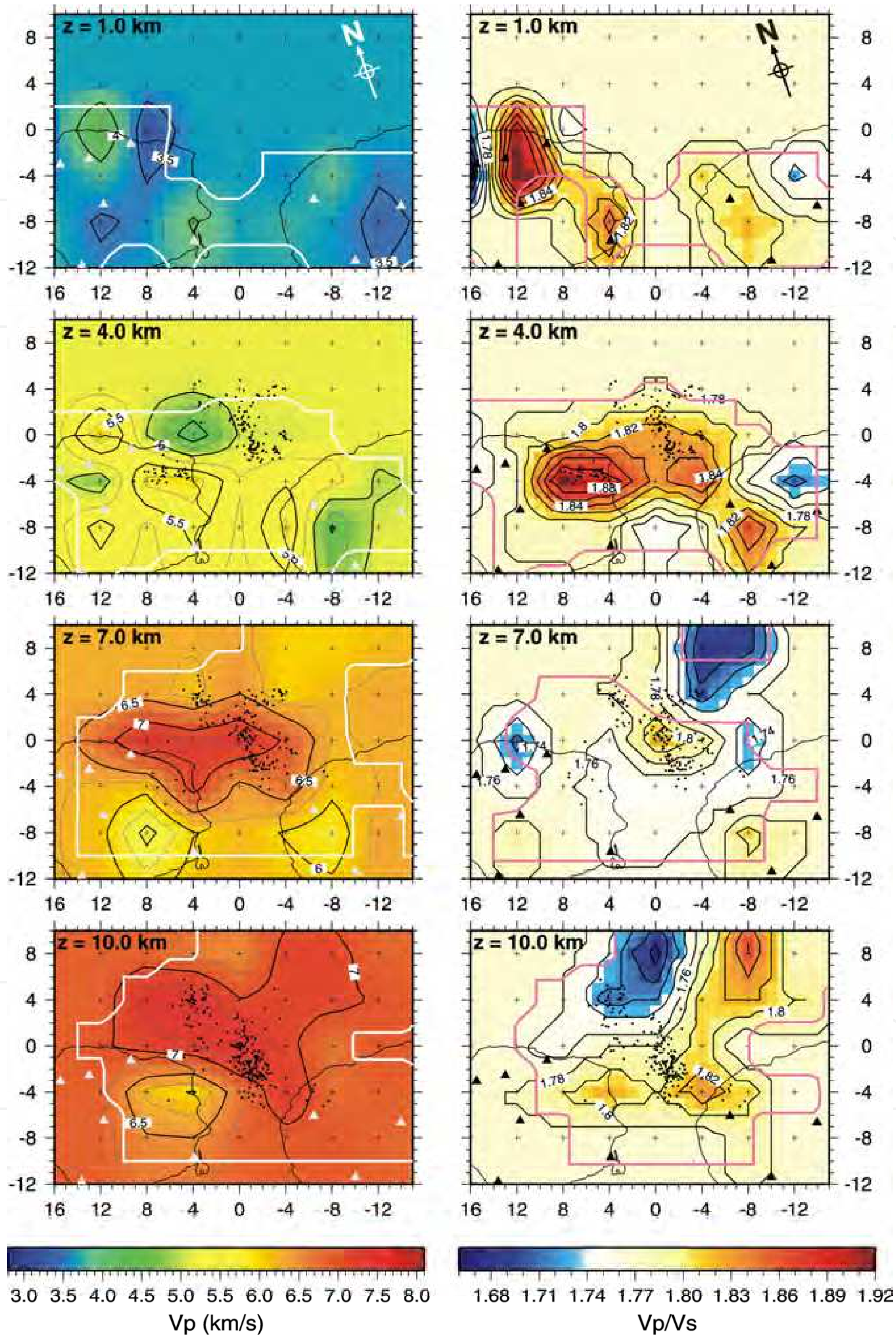

Fig. 4. Horizontal depth planes of the 3-D Vp (left) and Vp/Vs (right) models, at selected depths. Triangles: seismic stations, crosses: grid nodes, dots: epicenters within 1 km vertical range of the plane. Lateral XY coordinates according to the 3-D grid of Fig. 3.

Overall, the distribution of the observed seismicity is linked to areas of high value of the Vp/Vs ratio (> 1.84), also linked in some places to the high values of Vp, which should reflect changes in the mechanical properties of the rocky surroundings in fault areas.

4. Hypocentral relocation

The accurate determination of an earthquake hypocenter parameters, that is geographical coordinates, focal depth and time of occurrence, requires some knowledge on the crustal structure between the seismic focus and the receiving station. With the knowledge of such structure, usually parameterized in a seismic velocities model, the space-time coordinates of an event can be determined from the observed arrival moments of the seismic waves recorded at several stations (inverse problem). Depending on the specific structure of the used velocity model, the hypocentral location and especially the determination of the focal depth can undergo major changes.

Regarding the aftershocks of the July 9th 1998 earthquake, the preliminary location made by SIVISA (cf. Fig. 1) was carried out using model MAC (Hirn et al., 1980; Senos et al., 1980). MAC is a 1-D model developed with the purpose of locating all offshore seismicity in the Azores region, and reflects the average crustal structure of the plateau. The determination of the new 1-D model of the Faial-Pico-São Jorge area and of the tomographic 3-D model automatically entails a revision of the seismic hypocentral parameters used in the modelling.

In mathematical terms, the relocations by the new 1-D and 3-D models leads to substantial reduction of the data root mean square (RMS): relatively to the MAC model the new 1-D model allows for a reduction of 63% of the RMS, from 0,286 s to 0,103 s, while the use of the 3-D model leads to a further reduction of 32% of this parameter reaching 0,070 s (75.5% compared to the MAC model). In spatial terms, the changes entailed by the 1-D modelling generally do not exceed 2 km shifts of the epicentral position (cf. Fig. 5), with an additional 1 km in the tomographic inversion. The changes in focal depths are more relevant because they reduce the thickness of the fragile layer to the upper 15 km (22 km with the MAC model).

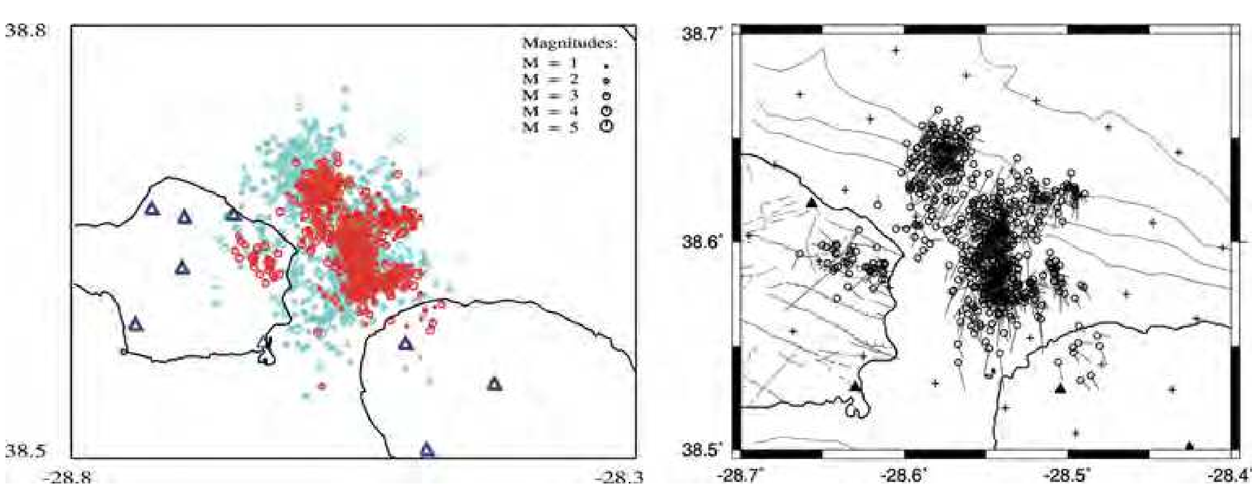

Fig. 5. Left: Comparison between the original epicenter locations (blue) of the 692 events with MAC model and the revised epicenter locations (red) with the new 1-D model FAIAL98. Right: Relocated events following the tomographic inversion; circles represent the final positions obtained with the 3-D model, line segments the position shift.

In terms of the seismicity spatial organization following the relocation (cf. Fig. 5), both models revealed two main alignments compatible with the two nodal planes of the focal mechanism of the main earthquake (cf. Fig. 1): one striking NNW-SSE, containing the majority of the aftershocks, and a secondary one with ENE-WSW direction. Most of the seismicity occurs in the Faial-Pico channel area, the inland events being less relevant both in terms of occurrence rates and magnitudes (Dias, 2005). This inland seismicity presents a NW-SE alignment, especially in Faial.

5. Seismic anisotropy and crustal stress

Seismic anisotropy is a three-dimensional phenomenon that takes different forms, corresponding to the variation in the wave's propagation velocity with azimuth and eventual splitting of an S-wave into several pulses (birefringence). The interpretation of the crustal seismic anisotropy is sometimes carried out according to the Extensive Dilatancy Anisotropy model (Crampin et al. 1984), which states that as result of a crustal stress field, a initially isotropic homogeneous medium undergoes micro-fracturing (or previously existing micro-fractures are reoriented), the assumed plane fractures adjusting to directions roughly parallel to the direction of maximum horizontal stress (and perpendicular to the direction of minimum horizontal stress). The presence of fluids in the crust (H_2O, CO_2) usually leads to the filling up of these micro-fractures, changing the propagation properties according to direction. An S-wave with sub-vertical incidence in such medium will split into two orthogonally polarized quasi-S-waves, propagating with different velocities due to the variations of the mechanical properties in the parallel and perpendicular directions to the micro-fractures. As a result seismic anisotropy will be observed, its level being evaluated from the measurement of the time difference between the arrivals of these two S-waves.

Following the method of Bouin et al. (1996) 438 events were selected, the analysis of their records suggesting signs of anisotropy. Although the 3D revised hypocenters solutions are more accurate, the error involved in the measurement of the splitting directions allows using the simpler 1D approach: the already referred sampling rate of 62.5 Hz, for the data stored for the majority of the digital temporary stations, coupled with the difficulties in the north alignment of the seismic sensors in basaltic oceanic islands, outmanoeuvre the accuracy of using 3D locations instead of 1D. On the other hand, most of the programs available for crustal stress modelling are 1D based (Robinson & McGinty, 2000).

The detection and quantification of such anisotropy was possible only in some of the digital stations located on the islands of Faial and Pico (cf. Fig. 6). In each station, the presence of anisotropy in the S-wave window records was shown by a systematic polarization of the first pulse of this kind of wave, sometimes followed by a second pulse showing a roughly orthogonal polarization. Figure 6 represents the results obtained for each station, with the rose diagrams representing the statistical direction of polarization of the first (blue) and second (red) S-waves. In a general, the observed polarization is very stable and independent of the epicentral distribution, ranging from approximately NW-SE direction in the northern Faial and north-western Pico to a significantly orthogonal WSW-ENE direction in the eastern area of Faial island.

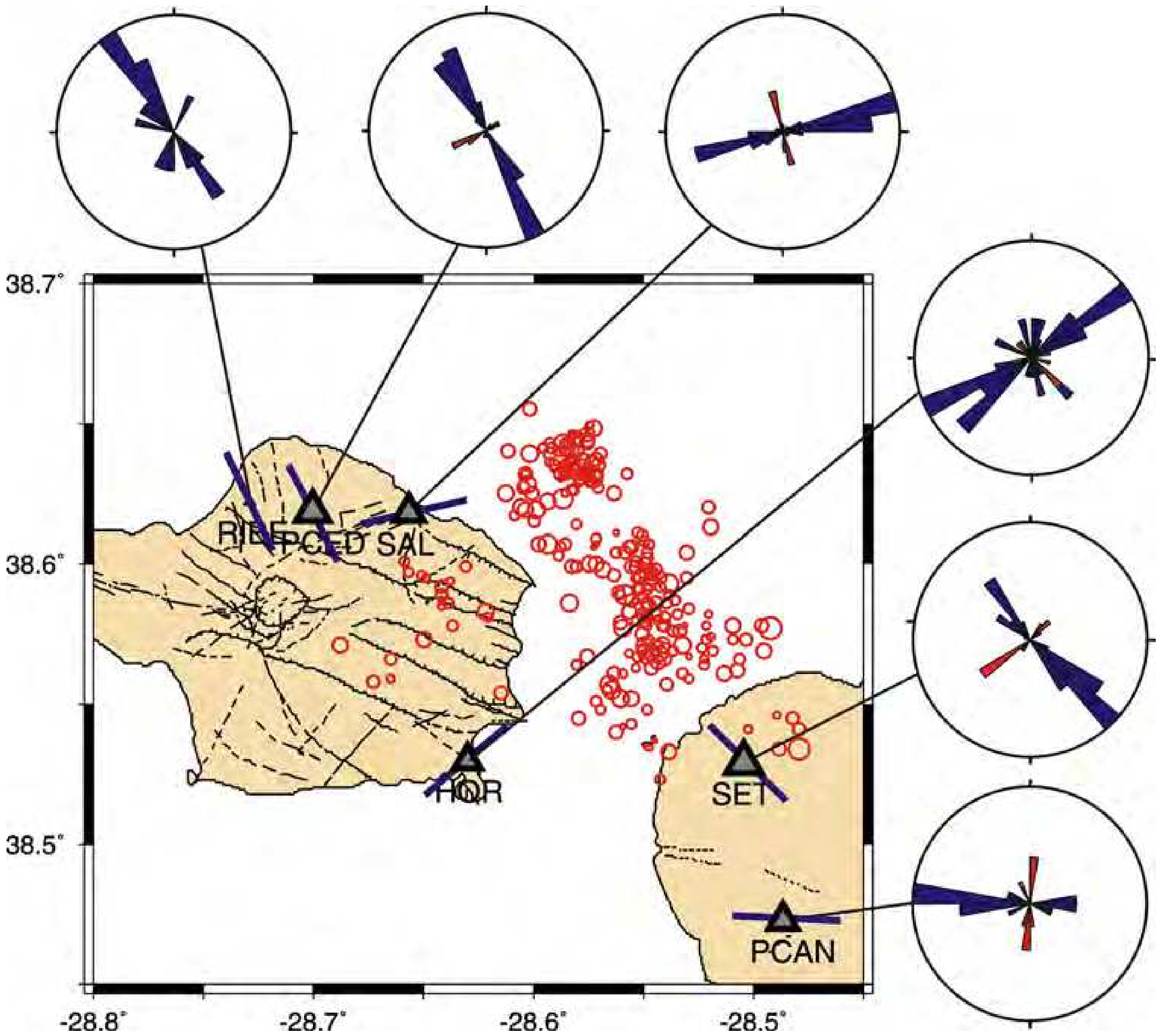

Fig. 6. Epicenters of the 438 selected events together with rose diagrams (10º intervals) of the polarizations directions, as measured in each station, of the fast (blue) and slow (red) S-waves. The size of each station symbol is proportional to the respective quantified anisotropy level, with the mean polarization direction of the fast S-wave projected over each station.

To relate the crustal stress state in the area affected by the seismic crisis, there are two seismologic indicators to determine the direction of maximum horizontal stress, SHmax or σ1: the analysis of the polarization of the S-wave and the computation of focal mechanisms. The markers associated with focal mechanisms (usually the direction of the P axis) reflect the state of stress in the source area, while the direction of polarization of the first wave associated with the birefringence of S-waves reflects the direction of maximum horizontal stress in the shallower structure located beneath the station. In case of focal mechanisms, single or composed, the estimate of SHmax is made according to the criteria defined by Zoback (1992), which relates the orientation of tension T or pressure P axis with the direction of SHmax.

To calculate single focal mechanisms, 18 events were selected with a minimum of 11 polarities for the P-wave, the hypocentral location used in calculating the focal parameters obtained from the 1-D model FAIAL98 (Matias et al., 2007). In the case of composite focal mechanisms, a similarity analysis of the recorded waveforms was performed by cross-correlation, which established a classification of "similar" earthquake clusters; subsequently, the joint focal mechanism was calculated for the 16 more numerous and stable clusters (Dias, 2005). The compilation of these results is represented in Figure 7 together with the estimated SHmax direction for both indicators.

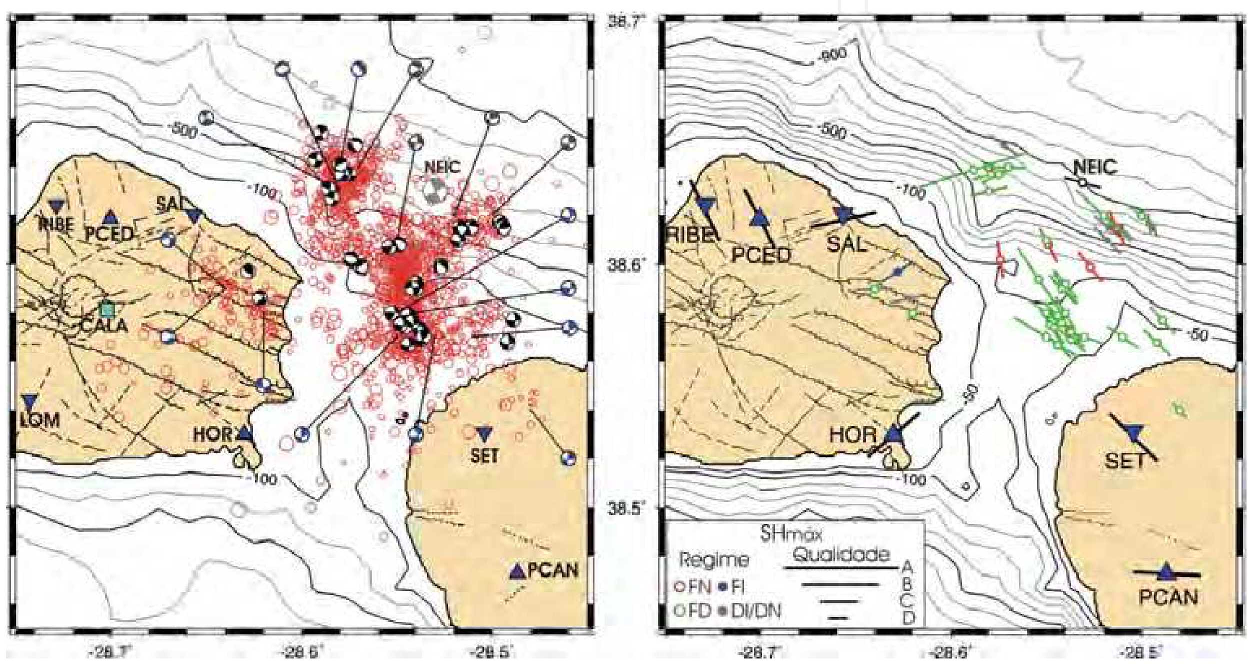

Fig. 7. Left: Aftershocks distribution of 9-7-1998 main shock, for events recorded by at least - 4 stations readings and relocated with the 1-D model FAIAL98; single (black) and composite (grey) focal mechanisms, together with the Harvard-CMT solution for the main shock. Right: maximum horizontal stress (SHmax) directions obtained from focal mechanisms and S-waves polarization analysis. The segments length is proportional to the quality of the stress measurement following Zoback (1992). The regime indicates the focal mechanism type: FN - normal fault, FD - stryke-slip fault, FI – inverse fault, DI/DN –oblique fault with inverse/normal component. Batimetry of Lourenço et al. (1998).

Figure 7 shows two dominant almost orthogonal general orientations for the maximum horizontal stress, N220ºE -N260°E and N90ºE-N130°E, limited to two distinct areas, with an apparent sharp transition of SHmax between them. As this indicator corresponds to the horizontal projection (i.e. two-dimensional) of a three-dimensional crustal stress vector, this sharp transition may be apparent, since the horizontal projection of T and P axis of the focal mechanisms suggests a continuous rotation (albeit fast) in the orientation of these axis (Dias, 2005).

The orientations obtained for the dominant polarization directions show some correlation with the tectonic alignments of Faial and Pico, which could suggest a tectonic control of the crustal fracturing near the stations. The observed anisotropy is consistent with the presence beneath the stations of anisotropy of the type envisaged by the EDA model, with the crack planes parallel to the direction of maximum horizontal stress. The major uncertainty is related with the depth extension of the anisotropic structures. The estimated directions for the maximum horizontal stress (SHmax), obtained from single and composed focal mechanisms solutions, is around 50º-80º in the NE zone of the Faial island, and a SHmax direction of around 130º-140º for the NW area of Pico island. The different orientations in the polarization direction obtained for the stations located in the north of Faial appears to be also related with the effect observed in the macroseismic effects (substantial mitigation of intensities) and the blocking of the progression of seismic activity to NW (Matias et al., 2007).

6. Coulomb stress variation

The aftershock distribution (Fig. 5) presents an odd distribution, with events aligned along roughly perpendicular directions, and the area surrounding the main shock seems to be devoided of significant aftershock activity. Furthermore, the focal mechanisms obtained from the best-constrained aftershocks indicate both strike-slip and normal faulting, suggesting that different faults have ruptured after the main shock.

Following the revision by Das & Henry (2003) on the relationship between the main earthquake slip and its aftershock distribution, the occurrence of low magnitude events in the high-slip regions of the fault that ruptures is rare. Instead, the authors have found that, in most cases, the aftershocks occur in nearby faults that are reactivated by a favourably oriented post-seismic static stress.

To investigate this possibility we have used the method implemented in the program GNStress (Robinson & McGinty, 2000), that calculates the crustal strains and their derivatives in a homogeneous half-space due to slip in a rectangular fault. To convert strains to stresses in the half-space a constant rigidity of 2.68×10^{10} Pa was used. A regional stress field with $\sigma 1$ (maximum compressive stress) oriented N135E, was assumed according to the transtensional tectonic regime deduced for this area of the Azores archipelago from neotectonic investigation (Madeira & Ribeiro, 1990). For the main shock source description we used the parameters derived from GPS data (Fernandes et al., 2002), namely the solution of a rectangular fault 9 km long x 4.5 km wide, oriented N165E, with the top of the fault plane lying 2 km below the topographic zero. A detailed discussion of the procedure can be found in Matias et al. (2007).

The calculated distribution of the Coulomb failure stress is presented in Fig. 8. Looking at the depth distribution of the variation in the Coulomb failure stress, and its relationship with aftershock distribution, we conclude that the main shock ruptured a very shallow fault, from a depth of 2 to 7 km, and then most of the aftershocks occurred below this depth along faults that were favourably orientated in relation to the post-seismic stress field. This very simple model doesn't explain the shallowest activity, above 7 km depth. It may be a consequence of the simple half-space model assumed for the stress computations.

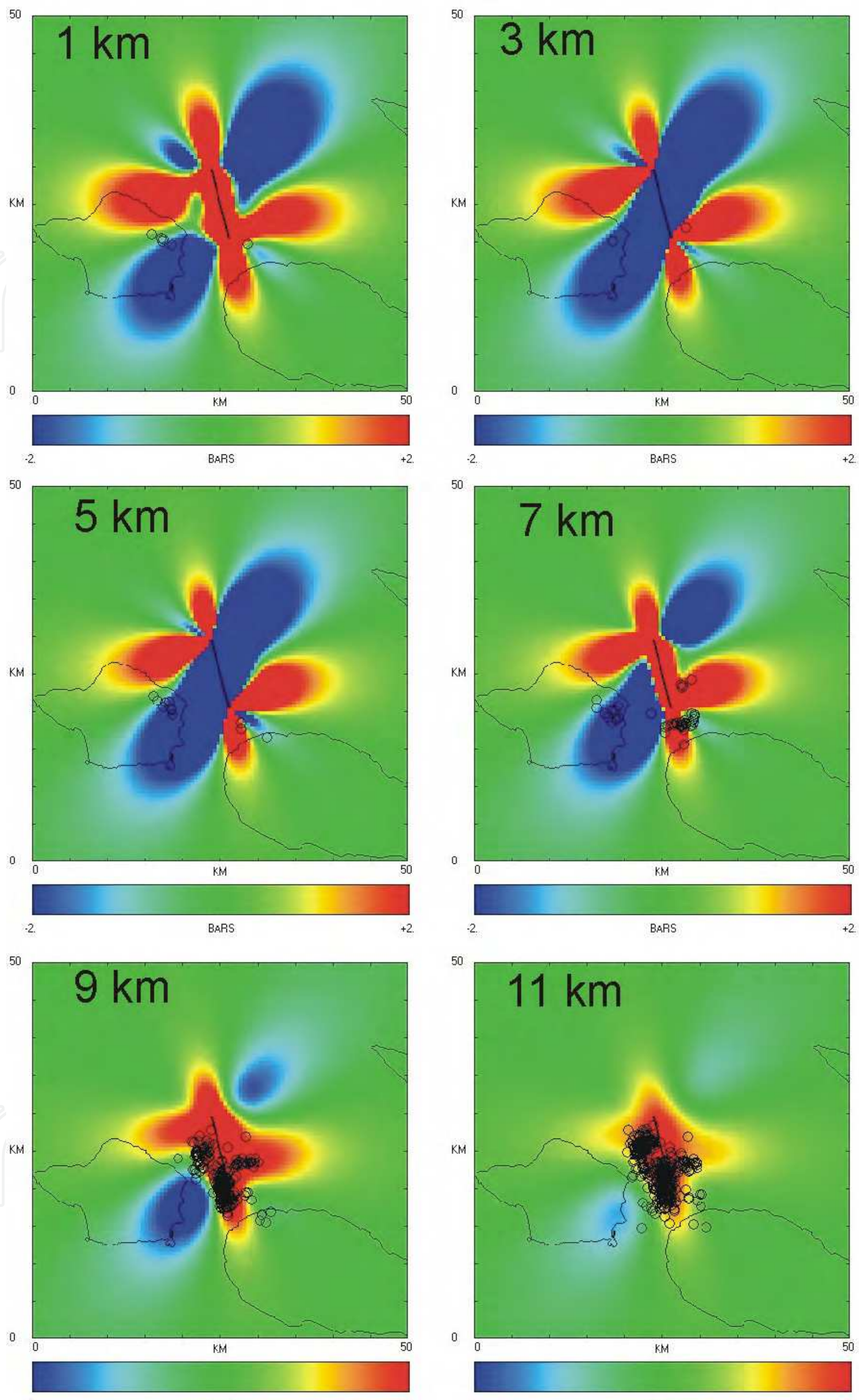

Fig. 8. Induced changes in Coulomb failure stress (δCFS) due to the main shock and its comparison to aftershock distribution. The δCFS was computed for 6 reference depths: 1, 3, 5, 7, 9 and 11 km. The aftershocks were plotted according to the depth ranges. The assumed main shock source plane is indicated in each figure.

7. Conclusion

The results obtained from the 1-D and 3-D inversions allow an insight of the crustal structure of the Azorean plateau region, primarily in the Central Group area between the islands of Faial and Pico. In terms of crustal thickness, the 1-D model points to a Moho located at 12.5 km depth while the 3-D model, though not allowing an evident definition in the velocities transitions, corroborates this suggestion with the Vp = 7.8 km/s isoline fluctuating around 14 km depth. Although this crustal thickness is higher than those determined in other studies, pointing to values around 8-11 km (Luis et al., 1998; Miranda et al., 1998; Luis & Neves, 2006), these works were performed at the plateau scale or in offshore areas while the models presented here necessarily include the structure of the islands (where the stations are located), thus justifying a further thickness increase of about 2-3 km. Additionally, a crustal thickness of 14 km fits better the estimated parameters for the largest instrumental earthquakes, both in terms of the sources estimated geometry and the correlation with the recorded magnitudes (Madeira et al., 2003).

The resulting distribution of seismicity indicates that for the main observable tectonic structures, the most active corresponds to the one of NNW-SSE orientation with the focal mechanisms indicating a dominant left strike-slip movement, with a secondary WSW-ENE direction of dominant right strike-slip. The NW-SE structures have a minor role, mainly confining seismicity.

The presence of seismic anisotropy was detected beneath the seismic stations (cf. Fig. 6), compatible with the EDA model, with a correspondence between the fracturing index and the positioning of each station. The estimated orientation for the direction of maximum horizontal stress from the S-wave polarization analysis, combined with single and composite focal mechanisms solutions, indicates a complex pattern in the crustal stress paths rotating from a general NW-SE direction to NE-SW in the eastern section of the island of Faial and extending into the sea. The comparison with the crustal stress distribution at the shallow layer of 1 km depth (cf. Fig. 8), shows that the measured direction of polarization of the first (fast) S-wave appear to follow the lobules shape, at least in northern Faial (RIBE, PCED, SAL stations) and NW Pico island (SET station). As for HOR station, in SE Faial island, is inside a low stress lobule and the polarization direction appears not to be correlated with the stress distribution although as it can be seen from Fig. 6, this station shows a bigger fluctuation in the measurements of the first polarization.

Comparing the distribution of seismicity and the rotation of SHmax direction (Fig. 5 and 7) with the tomographic model (Fig. 4), there is an apparent tectonic control by the high-velocity intrusion lying NE of Faial. It is essentially a crustal asseismic area enclosed by more active seismogenic areas, its form "conditioned" by the distribution of seismicity; in addition, the rotations in the directions of SHmax appeared to be sub-paralleled to the limits of this anomaly. Comparing with the Coulomb failure stress (cf. Fig. 8) planes coincident with the location of the main seismicity (layers between km depth) the SHmax directions show good correlation with the lobules shape, namely the rotation observed between NNW-SSE and WSW-ENE directions. The main exceptions appear to be the shallow seismicity observed inland in NE Faial island, in the area of Faial Graben.

The results shown here suggest a crustal thickening due to an increase in thickness of layer 3, the 1-D model presenting a total thickness of 9.5 km. This indicates that the accretion of the crust in the Azores plateau was essentially due to a relatively high magmatic supply rate, which cooled and crystallized at depth, with the rate of extruded volcanism though important playing a small role in the crustal build-up. The source of such high magmatism is still a matter under debate, maybe the result of the actual presence of a "hot-spot" in the Azores or, alternatively, be only the result of the condition of the plateau as a tectonic triple junction.

The mentioned presence of a high seismic waves velocity volume, interpreted as a crystalline intrusion of mafic (Gabbro) and ultra-mafic rocks, apparently constraining the observed seismicity and stress state, appears to corroborate the last assumption. Under the main volcanic edifices of Faial and Pico there is no clear signal of the presence of magmatic chambers, but this maybe result of to the poor coverage of seismic paths; the presence of a low-velocity anomaly is revealed, but this may be due only to the effect of a volcanic feeding system and not the presence of a magmatic chamber, something that concurs with the suggestion of Nunes et al. (2006) of a lack of magmatic chamber under Pico's volcano.

8. Acknowledgments

We would like to acknowledge the effort of all the people involved in the seismic monitoring campaign that took place in the Azores during July 1998, namely, C. Corela, A. Carvalho, and J. Simões. The figures were produced using the GMT software (Wessel and Smith 1991) and SEISAN software (Havskov and Ottemöller 1999).This work was supported by the Portuguese Fundação para a Ciência e Tecnologia, under projects MASHA (POCTI/CTA/39158/2001) and STAMINA (PDCTM1999MAR15255). Nuno A. Dias had a fellowship under the PRODEP III program, Action 5.3. This is a contribution to PEST-OE/CTE/LA0019/2011 – IDL.

9. References

Bouin, M.P., Tellez, J. & Bernard, P. (1996). Seismic anisotropy around the Gulf of Corinth, Greece, deduced from three-component seismograms of local earthquakes and its relationship with crustal strain. *Journal of Geophysical Research,* 101(B3), pp. 5797-5811.

Crampin, S., R. Evans & B.K. Atkinson (1984). Earthquake Prediction - a New Physical Basis. *Geophysical Journal of the Royal astronomical Society*, 76(1), pp. 147-156.

Das, S. & Henry, C. (2003). Spatial relation between main earthquake slip and its aftershock distribution. *Reviews of Geophysics*, 41(3), pp. 1013-1036.

Dias, N.A. (2005). Estudo da sequência sísmica gerada pelo sismo do Faial de 9 de Julho de 1998: anisotropia crustal, inversão tomográfica e caracterização sismo-tectónica. *PhD Thesis* (in Portuguese), Lisbon University, Lisboa, 540 pp.

Dias, N.A., L. Matias, N. Lourenco, J. Madeira, F. Carrilho & J.L. Gaspar (2007). Crustal seismic velocity structure near Faial and Pico Islands (AZORES), from local earthquake tomography. *Tectonophysics*, 445(3-4), pp. 301-317.

Eberhart-Phillips, D. (1993). Local earthquake tomography: earthquake source regions. In: H.M. Iyer and K. Hirahara (Editors), Seismic Tomography: Theory and practice. Chapman & Hall, London, pp. 613-643.

Fernandes, R.M.S., Miranda, J.M., Catalao, J., Luis, J.F., Bastos, L. & Ambrosius, B.A.C. (2002). Coseismic displacements of the M-W=6.1, July 9, 1998, Faial earthquake (Azores, North Atlantic). *Geophysical Research Letters*, 29(16), pp. 21 1-4.

Havskov, J. & Ottemöller, L. (1999). Seisan earthquake analysis software. *Seismological Research Letters*, 70, pp. 532-534.

Hirn, A., H. Haessler, P. Hoangtrong, G. Wittlinger & L.A. Mendes-Victor, 1980. Aftershock Sequence of the January 1st, 1980, Earthquake and Present-Day Tectonics in the Azores. *Geophysical Research Letters*, 7(7), pp. 501-504.

Karson, J.A. (1998). Internal Structure of Oceanic Lithosphere: A Perspective from Tectonic Windows. In: W.R. Buck, P.T. Delaney, J.A. Jeffery A. Karson and Y. Lagabrielle (Editors), Faulting and Magmatism at Mid-Ocean Ridges. Geophysical Monograph. American Geophysical Union, Washington, D.C., pp. 177-218.

Kissling, E. (1995). Program VELEST user's guide - Short introduction, ETH Zuerich, pp. 26.

Kissling, E., W.L. Ellsworth, D. Eberhart-Phillips & U. Kradolfer (1994). Initial Reference Models in Local Earthquake Tomography. *Journal of Geophysical Research,* 99(B10), pp. 19635-19646.

Kissling, E., S. Husen & F. Haslinger (2001). Model parametrization in seismic tomography: a choice of consequence for the solution quality. *Physics of the Earth and Planetary Interiors.*, 123(2-4), pp. 89-101.

Lourenço, N., J.M. Miranda, J.F. Luis, A. Ribeiro, L.A.M. Victor, J. Madeira & H.D. Needham (1998). Morpho-tectonic analysis of the Azores Volcanic Plateau from a new bathymetric compilation of the area. *Marine Geophysical Researches*, 20(3), pp. 141-156.

Luis, J.F., J.M. Miranda, A. Galdeano & P. Patriat (1998). Constraints on the structure of the Azores spreading center from gravity data. *Marine Geophysical Researches*, 20(3), pp. 157-170.

Luis, J.F. & Neves, M.C. (2006). The isostatic compensation of the Azores Plateau: A 3D admittance and coherence analysis. *Journal of Volcanology and Geothermal Research*, 156(1-2), pp. 10-22.

Machado, F., Matias, L. & Lemos, A. (1994). Vibration of magma under the volcano of Pico (Azores Islands). Acta Vulcanologica, 5, pp. 147-151.

Madeira, J. & Ribeiro, A. (1990). Geodynamic Models for the Azores Triple Junction - a Contribution from Tectonics. *Tectonophysics*, 184(3-4), pp. 405-415.

Madeira, J. & Silveira, A.B. (2003). Active tectonics and first paleoseismological results in Faial, Pico and S. Jorge Islands (Azores, Portugal). *Annals of Geophysics*, 46(5), pp. 733-761.

Matias, L., Dias, N., Morais, I., Vales, D., Carrilho, F., Madeira, J., Gaspar, J., Senos, L. & Silveira, A. (2007). The 9th of July 1998 Faial Island (Azores, North Atlantic) seismic sequence. *Journal of Seismology*, 11(3), pp. 275-298.

Menke, W., 1984. Geophysical Data Analysis: Discrete Inverse Theory. Academic Press, 260 pp.

Miranda, J.M., Victor, L.A.M., Simoes, J.Z., Luis, J.F., Matias, L., Shimamura, H., Shiobara, H., Nemoto, H., Mochizuki, H., Hirn, A. & Lepine, J.C. (1998). Tectonic setting of the Azores Plateau deduced from a OBS survey. *Marine Geophysical Researches*, 20(3), pp. 171-182.

Nunes, J.C., A. Camacho, Z. Franca, F.G. Montesinos, M. Alves, R. Vieira, E. Velez & E. Ortiz (2006). Gravity anomalies and crustal signature of volcano-tectonic structures of Pico Island (Azores). *Journal of Volcanology and Geothermal Research*, 156(1-2), pp. 55-70.

Robinson, R. & McGinty, P.J. (2000). The enigma of the Arthur's Pass, New Zealand, earthquake 2. The aftershock distribution and its relation to regional and induced stress fields. *Journal of Geophysical Research*, 105(B7), pp. 16139-16150.

Senos, M.L., J.C. Nunes & V.S. Moreira (1980). Estudos da estrutura da crosta e manto superior nos Açores, INMG, Lisboa.

Tanimoto, T. (1995). Crustal structure of the Earth. In: T. Ahrens (Editor), A Handbook of Physical Constants: Global Earth Physics. AGU Reference Shelf Series. AGU, pp. 214-224.

Thurber, C. & D. Eberhart-Phillips (1999). Local earthquake tomography with flexible gridding. *Computers & Geosciences*, 25(7), pp. 809-818.

Thurber, C.H. (1983). Earthquake Locations and 3-Dimensional Crustal Structure in the Coyote Lake Area, Central California. *Journal of Geophysical Research,* 88(B10), pp. 8226-8236.

Thurber, C.H. (1993). Local earthquake tomography: velocities and Vp/Vs - theory. In: H.M. Iyer and K. Hirahara (Editors), Seismic Tomography: Theory and practice. Chapman & Hall, London, pp. 563-583.

Thurber, C.H. (2003). Seismic tomography of the lithosphere with body waves. *Pure and Applied Geophysics*., 160(3-4), pp. 717-737.

Thurber, C.H. & Kissling, E. (2000). Advances in travel-time calculations for three-dimensional structures. In: C.H. Thurber and N. Rabinowitz (Editors), Advances in Seismic Event Location. Modern Approaches in Geophysics. Kluwer, Dordrecht, pp. 71-100.

Wessel, P. & Smith, W.H.F. (1991). Free software helps map and display data. EOS Trans. Amer. Geophys. U., 72(41), pp. 441 e 445-446.

Zoback, M.L. (1992). 1st-Order and 2nd-Order Patterns of Stress in the Lithosphere - the World Stress Map Project. *Journal of Geophysical Research,* 97(B8), pp. 11703-11728.

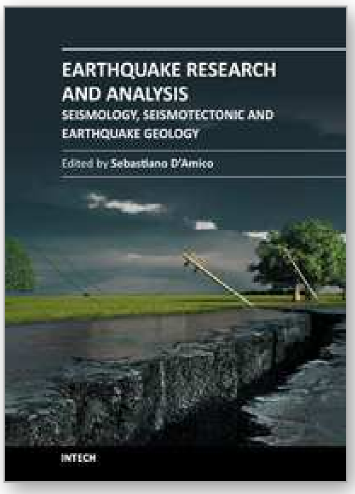

Earthquake Research and Analysis - Seismology, Seismotectonic and Earthquake Geology

Edited by Dr Sebastiano D'Amico

ISBN 978-953-307-991-2
Hard cover, 370 pages
Publisher InTech
Published online 08, February, 2012
Published in print edition February, 2012

This book is devoted to different aspects of earthquake research. Depending on their magnitude and the placement of the hypocenter, earthquakes have the potential to be very destructive. Given that they can cause significant losses and deaths, it is really important to understand the process and the physics of this phenomenon. This book does not focus on a unique problem in earthquake processes, but spans studies on historical earthquakes and seismology in different tectonic environments, to more applied studies on earthquake geology.